

Review

# Solid State Hydrogen Storage in Alanates and Alanate-Based Compounds: A Review

Chiara Milanese <sup>1,\*</sup> , Sebastiano Garroni <sup>2</sup> , Fabiana Gennari <sup>3</sup>, Amedeo Marini <sup>1</sup>, Thomas Klassen <sup>4,5</sup>, Martin Dornheim <sup>4</sup> and Claudio Pistidda <sup>4</sup> 

<sup>1</sup> Pavia Hydrogen Lab, C.S.G.I. & Chemistry Department, University of Pavia, Viale Taramelli, 16, 27100 Pavia, Italy; amedeo.marini@unipv.it

<sup>2</sup> International Research Centre in Critical Raw Materials-ICCRAM, University of Burgos, 09001 Burgos, Spain; sebastiano.garroni@gmail.com

<sup>3</sup> National Council of Scientific and Technological Research (CONICET), Bariloche Atomic Center (National Commission of Atomic Energy) and Balseiro Institute (University of Cuyo) Av. Bustillo 9500, San Carlos de Bariloche, Río Negro 8400, Argentina; gennari@cab.cnea.gov.ar

<sup>4</sup> Institute of Materials Research, Helmholtz-Zentrum Geesthacht, Max-Planck-Straße 1, D-21502 Geesthacht, Germany; thomas.klassen@hzg.de or klassen@hsu-hh.de (T.K.); martin.dornheim@hzg.de (M.D.); claudio.pistidda@hzg.de (C.P.)

<sup>5</sup> Institute of Materials Technology, Helmut Schmidt University, University of the Federal Armed Forces, Holstenhofweg 85, D-22043 Hamburg, Germany

\* Correspondence: chiara.milanese@unipv.it; Tel.: +39-0382-987-670

Received: 20 June 2018; Accepted: 18 July 2018; Published: 24 July 2018



**Abstract:** The safest way to store hydrogen is in solid form, physically entrapped in molecular form in highly porous materials, or chemically bound in atomic form in hydrides. Among the different families of these compounds, alkaline and alkaline earth metals alumino-hydrides (alanates) have been regarded as promising storing media and have been extensively studied since 1997, when Bogdanovic and Schwickardi reported that Ti-doped sodium alanate could be reversibly dehydrogenated under moderate conditions. In this review, the preparative methods; the crystal structure; the physico-chemical and hydrogen absorption-desorption properties of the alanates of Li, Na, K, Ca, Mg, Y, Eu, and Sr; and of some of the most interesting multi-cation alanates will be summarized and discussed. The most promising alanate-based reactive hydride composite (RHC) systems developed in the last few years will also be described and commented on concerning their hydrogen absorption and desorption performance.

**Keywords:** alanates; metal aluminum hydrides; solid state hydrogen storage; complex hydrides; reactive hydride composite

## 1. Introduction

Hydrogen is regarded as an efficient energy storage medium and a green and environmental friendly fuel able to help improve environmental issues linked to the use of fossil fuels [1,2], thanks to its high gravimetric energy density (more than twice the energy content of the most common fossil fuels) and its clean combustion reaction (leading to the formation of water only). Unfortunately, its volumetric capacity is very low, leading to the well-known storage problems [2]. The safest method to store hydrogen is in solid state form, that is, bound to a solid as molecules through physical interactions (physisorption) or in atomic form by chemical bonds (chemisorption). The most promising materials for hydrogen storage concerning the gravimetric and volumetric capacity belong to this last group, suffering anyway from unfavourable working conditions (i.e., high temperature and hydrogen pressure) and scarce cycling ability [1]. The first system to be considered interesting for

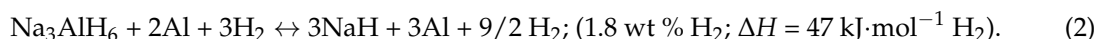
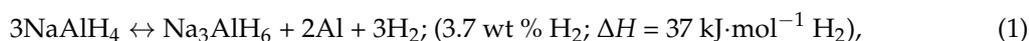
practical applications, thanks to its reversibility in exchanging hydrogen at moderate temperature and pressure conditions, was based on an alanate, that is, titanium-based doped sodium alanate, studied by Bogdanovic and Schwickardi in 1996 [3]. The term ‘alanate’, synonymous of ‘aluminio-hydride’, refers to a family of complex hydrides, in which a metallic cation coordinates, with an ionic bond, an anion with Al in the center, covalently binding four hydrogen atoms. Since Bogdanovic’s discovery, many efforts have been made to investigate the hydrogen absorption and desorption mechanism of Na alanate and of the other alkaline and alkaline earth metal alanates, and to optimize their performance by doping with suitable catalysts and destabilizing agents, by wet chemistry infiltration and by mixing in the so-called reactive hydride composite (RHC) approach. Recently, some of them have also been proposed for electrochemical applications in solid state ion batteries. In this review, the preparative methods; the crystal structure; the physico-chemical characteristics; the hydrogen absorption and desorption properties of the alanates of Li, Na, K, Ca, Mg, Y, Sr, and Eu; and the hydrogen absorption and desorption properties of the most appealing multi-cations alanates and of selected systems based on these compounds will be summarized and discussed. The most promising alanate-based RHC systems developed in the last few years will also be described and commented.

## 2. Alanates Based-Systems

### 2.1. Sodium Alanate $\text{NaAlH}_4$

A direct synthesis of  $\text{NaAlH}_4$  from sodium hydride, aluminium, and hydrogen under pressure in several different solvents was described in the early sixties by Ashby et al. and Clasen [4,5]. Dymova et al. [6] proposed a synthetic procedure from the elements at temperatures lower than 553 K and hydrogen pressure of 175 bar. The alanate can be easily prepared contextually with its doping with metals by ball milling under inert atmosphere, via wet chemistry reaction of a  $\text{NaH-Al}$ -dopant powder mixture and subsequent hydrogenation [7], or by one-step direct synthesis by high energy reactive ball milling [7,8]. The crystal structure of  $\text{NaAlH}_4$ , determined by single crystal X-ray diffraction, is tetragonal with space group  $I4_1/a$ , consisting of isolated  $[\text{AlH}_4]^-$  tetrahedra [9]. The Al–D bond length, evaluated more recently by neutron diffraction on the deuterated compound at 295 K, is 1.6262 Å, while the two Na–D distances are 2.431(2) Å and 2.439(2) Å. The shortest (Al–Al) distance is 3.779(1) Å. The angles of the  $[\text{AlD}_4]$  tetrahedron are distorted and equal to 107.32° and 113.86° [10].

$\text{NaAlH}_4$ , with 5.5 wt %  $\text{H}_2$  theoretical gravimetric capacity and 5.0 wt % hydrogen release reached so far, is amongst the most advanced and intensely investigated materials for hydrogen storage; even if it seems evident that its performance will be not suitable for on-board applications, it is considered promising for stationary purposes [11]. Its dehydrogenation takes place in two steps [12,13]:



The activation energies for the two steps are 118 and 124  $\text{kJ}\cdot\text{mol}^{-1} \text{ H}_2$  [14], respectively. The further dissociation of NaH, responsible of the release of 1.9 wt %  $\text{H}_2$ , takes place above 723 K, making this last process unsuitable for practical applications. The equilibrium pressure calculated from the enthalpy values is 1 bar at 303 K for the first step and at 373 K for the second step respectively, making only reaction (1) useful to feed a proton exchange fuel cell membrane under full throttle conditions (353 K maximum) from a thermodynamic point of view. Considering the kinetic aspects, both reactions (1) and (2) are very slow for practical applications; Ashby and Kobetz [15,16] reported that the formation of  $\text{Na}_3\text{AlH}_6$  from  $\text{NaAlH}_4$  takes place in 3 h at 483–493 K, while to obtain an appreciable speed for the dissociation of the newly formed compound, temperatures higher than 523 K are required. Concerning re-hydrogenation, complete conversion from NaH and Al to  $\text{NaAlH}_4$  was achieved by Dymova et al. [6] in 3 h under 175 bar hydrogen pressure at 543 K. In 1997, Bogdanovic and co-workers [3] demonstrated that the kinetics of the system could be strongly improved by metal doping, in particular by adding

a few molar percent of Ti, and that the system could be reversibly operated under practical conditions. In these conditions, the activation energies of the two steps reduced to 80 and 96  $\text{kJ}\cdot\text{mol}^{-1}$   $\text{H}_2$ , and the isotherm of the re-absorption of hydrogen followed the desorption isotherm with almost no hysteresis. Anyway, the hydrogenation and dehydrogenation rates of the catalyzed systems are still insufficient for practical applications. Moreover, most of the catalysts were found to react with the hydrides, decreasing the gravimetric capacity of the systems and their whole storage performance.

Starting from the results of this work, many Ti-containing compounds (i.e.,  $\text{TiF}_3$ ,  $\text{Ti}(\text{OBu})_4$ ,  $\text{TiH}_2$ , and  $\text{TiO}_2$ ) were tested as catalyst, but by-side reactions with formation of compounds in which Ti combines with Al [11] were always observed, wasting the hydrogen absorption and desorption performance [17]. Considering the kinetics of the reactions, a linear increase of the rate as a function of the added amount of the Ti-compounds was recorded up to 5 mol % of catalyst in the active phase. For highest amounts, no variation in the reaction speed was noticed.

Concerning other transition metal salts, the addition of 2 mol % of  $\text{ScCl}_3$  and  $\text{CeCl}_3$  to  $\text{NaAlH}_4$  almost halves the re-hydrogenation times at high pressures and reduces them by a factor of ten at low pressures [14]. Moreover, these systems re-charged 3.5 wt % of hydrogen within 1 h at 50 bar, performance that is more promising than that of the titanium doped system. Zidan et al. [18] found zirconium addition acting in a very positive way towards reaction (2), leading to a reversibility higher than 4 wt %. Wang et al. [19], in their systematic study on the action of individual, binary, and ternary combinations of  $\text{TiCl}_3$ ,  $\text{FeCl}_3$ , and  $\text{ZrCl}_4$  on the dehydrogenation kinetics of the Na alanate, reported that the effect of the presence of more than one catalyst with respect to single doping was pronounced on reaction (1), but almost negligible on reaction (2). Lee et al. reported a noticeable improvement in the desorption kinetics of the alanate thanks to the addition of  $\text{La}_2\text{O}_3$  [20]. Further, C-based materials were tried as catalysts; Zaluska et al. first [21] succeeded in accelerating the dehydrogenation kinetics by ball milling the alanate with the addition of pure carbon. Pukazhselvan et al. have shown that  $\text{NaAlH}_4$  mixed with 8 mol % carbon nanotubes (CNTs) could reach a reversible hydrogen gravimetric capacity of 4.2 wt % with interesting kinetic performance [22], probably because of the improved solid-gas exchange consequent to the increase in the surface area of the catalysed material. According to Berseth et al. [23], when  $\text{NaAlH}_4$  interacts with an electronegative material such as carbon nanotubes, the charge donation ability of Na is affected, the Al–H bond results weakened, and the hydrogen release can take place at a lower temperature. Atakli et al. [24] constructed the Gibbs free energy diagrams for Na alanate and for other alkali metals alanates in order to determine the stability of reactants, intermediates, and products based on the previously published experimental thermodynamic data. All the investigated alkali alanates follow the same hydrogen desorption path: the hexahydride is formed by transferring the alkali cation  $\text{M}^+$  and a hydrogen anion  $\text{H}^-$  from the two neighboring alanates to the central one, leading to the formation of the hexahydride. The activation energy of the transfer of an alkali hydride MH is lower than the experimentally determined activation energy, while the transfer of  $\text{M}^+$  and  $\text{H}^-$  is energetically above the experimental value; this means that the extent of charge separation determines the activation energy. The role of the Ti catalyst is to reduce the charge separation by forming a bridge between  $\text{M}^+$  and  $\text{H}^-$ . In reaction (2), where the movement of an alkali hydride takes place, Ti acts to form the metal-hydrogen bridge too.

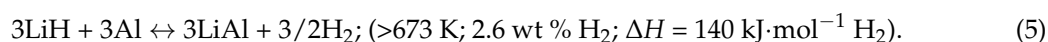
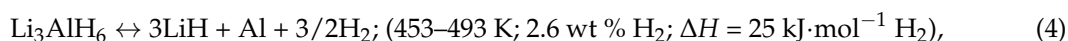
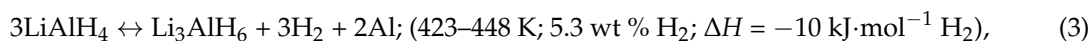
Ball milling the pure alanate is also a good strategy to improve the kinetics and to lower the desorption temperature. After 15 min of ball milling, the pure Na alanate releases up to 3.1 wt %  $\text{H}_2$  at 433 K, according to reaction (1), while an additional 1.9 wt % due to reaction (2) is released at 493 K [25]. Baldè et al. [26] showed that the desorption activation energy of the pure compound decreases from 116  $\text{kJ}\cdot\text{mol}^{-1}$  for 1–10  $\mu\text{m}$  particles down to 58  $\text{kJ}\cdot\text{mol}^{-1}$  for 2–10 nm particles; this last energy value is lower than that of Ti catalyzed  $\text{NaAlH}_4$ . Moreover, the same authors demonstrated that the alanate nanoparticles are already able to absorb hydrogen at pressures as low as 20 bar at 388 K.

## 2.2. Lithium Alanate $\text{LiAlH}_4$

Lithium alanate ( $\text{LiAlH}_4$ ) was synthesized for the first time in 1947 by dissolution of lithium hydride in an ether solution of aluminium chloride [27]. However, this process is not convenient because more than 75% of  $\text{LiH}$  converts in  $\text{LiCl}$  [28]. Ashby et al. [4] and Clasen [5] performed a synthesis using diethyl ether, tetrahydrofuran, and diglyme solution. Clasen worked at low pressure (30 bar) and temperature (308 K), while Ashby performed this reaction under 350 bar of hydrogen at 393 K. Wang et al. [29] realized a procedure in five steps to obtain crystalline  $\text{LiAlH}_4$  starting from  $\text{Li}_3\text{AlH}_6$ ,  $\text{LiH}$ , and  $\text{Al}$ . Kojima et al. [30] ball milled  $\text{LiH}$  and  $\text{Al}$  for 24 h under 10 bar hydrogen pressure at room temperature, but the amount of  $\text{LiAlH}_4$  produced was very low.

Sklar and Post [31], by single crystal X-ray diffraction (XRD), determined a monoclinic structure with space group  $P_{21}/c$  for Li alanate; in it, each Al atom is surrounded by four hydrogen atoms to form  $[\text{AlH}_4]^-$  tetrahedra with Al–H bond lengths equal to 1.55 Å.  $\text{Li}^+$  is surrounded by five hydrogen atoms; four at distances between 1.88 and 2.00 Å and a fifth one at 2.16 Å. Hauback et al. [32], performing XRD and neutron diffraction at 8 K and 295 K, saw the Li atoms bonded to one deuterium atom from each of five surrounding  $\text{AlD}_4$  tetrahedra and adopting trigonal bipyramidal coordination. The distortion in the tetrahedral configuration was found to be in agreement with the literature [31] and it increases by cooling. The Al–D distances are in the range of 1.603–1.633 Å at 295 K and 1.596–1.645 Å at 8 K.

$\text{LiAlH}_4$  has a theoretical gravimetric capacity of 10.5 wt %  $\text{H}_2$  and dehydrogenates in the following three steps [16,33,34]:



The first two steps lead to a total amount of hydrogen released equal to 7.9 wt %, which could be attractive for practical applications, but the working temperatures and the desorption kinetics are still far from the practical targets. Several strategies have been applied in the last few years to overcome these limits, such as ball-milling and catalysts additions [35–51]. As described for Na alanate, Ti-based compounds such as  $\text{TiO}_2$ ,  $\text{TiC}$ ,  $\text{TiF}_3$ ,  $\text{TiN}$ , and  $\text{TiCl}_3$  [35,38,42] work in improving the desorption performance, as well as for the Li compound. The high catalytic activity of  $\text{TiCl}_4$  is due to the formation of a nano- or microcrystalline  $\text{Al}_3\text{Ti}$  phase obtained by the reaction between  $\text{TiCl}_4$  and  $\text{LiAlH}_4$  upon milling [35]. C-materials, (including carbon nano fibers (CNFs), graphitic nano fibers (GNFs), single-walled carbon nanotubes (SWCNTs), and multi-walled carbon nanotubes (MWCNTs, [38,39,42,51]) and metal halides, such as  $\text{VBr}_3$ ,  $\text{VCl}_3$ ,  $\text{ZrCl}_4$ ,  $\text{NbF}_5$ ,  $\text{NiCl}_2$ , and  $\text{K}_2\text{TiF}_6$  [36,41–44] were claimed to be able to destabilize  $\text{LiAlH}_4$ , significantly reducing its dehydrogenation temperature in the different steps. Zhou et al. [36] demonstrated by temperature-programmed desorption (TPD) measurements that the onset dehydrogenation temperature of  $\text{CeF}_3$  doped  $\text{LiAlH}_4$  was sharply reduced by 90 K compared with that of pristine  $\text{LiAlH}_4$ . The dehydrogenation activation energies of the  $\text{CeF}_3$  doped  $\text{LiAlH}_4$  sample, based on differential scanning calorimetry (DSC) data by applying Kissinger method, were 40.9  $\text{kJ}\cdot\text{mol}^{-1} \text{ H}_2$  and 77.2  $\text{kJ}\cdot\text{mol}^{-1} \text{ H}_2$  for reaction (3) and (4), respectively, which means values about 40.0  $\text{kJ}\cdot\text{mol}^{-1} \text{ H}_2$  and 60.3  $\text{kJ}\cdot\text{mol}^{-1} \text{ H}_2$  lower than pure  $\text{LiAlH}_4$ , respectively.

It is worth noting here that when substances such as  $\text{MnFe}_2\text{O}_4$  [37],  $\text{TiC}$  [38,42],  $\text{TiF}_3$  [43,47],  $\text{TiO}_2$  [47],  $\text{Nb}_2\text{O}_5$  and  $\text{Cr}_2\text{O}_3$  [40],  $\text{Fe}$  [48],  $\text{NbF}_5$  [41],  $\text{NiCl}_2$ , and  $\text{TiN}$  [42,45] are added to  $\text{LiAlH}_4$ , the first dehydrogenation step (4) is found to be exothermic. For RE fluorides doped samples ( $\text{REF}_3$ , RE = Ce, Y and La) [36,43], the first dehydrogenation process is endothermic, which is in agreement with the results shown in the literature [44,45]. Chen et al. [46] claimed that reaction (4) is intrinsically endothermic and the addition of  $\text{REF}_3$  may help to reveal this endothermic nature by uncoupling it from the melting-decomposition-solidification process, evolving at 438 K and 453 K in the pristine  $\text{LiAlH}_4$ .

Ball milling  $\text{LiAlD}_4$  with  $\text{VCl}_3$  or  $\text{TiCl}_3 \cdot 1/3\text{AlCl}_3$  [47] or adding  $\text{LaCl}_3$  [48] to the pristine alanate decreased the decomposition temperature by about 50–60 K and 30 K, respectively. The effect of Ni nanoparticles as catalyst improves with the decreasing of the particle size [49]. The addition of  $\text{NiCl}_2$  in place of Ni leads to a stronger effect, decreasing the dehydrogenation temperature of even 50 K.

The addition of MWCNTs decreased the onset dehydrogenation temperature of  $\text{LiAlH}_4$  from 443 K down to 313 K (thermogravimetric analysis TGA). However, the onset dehydrogenation temperature was shifted to 463–473 K if MWCNTs were decorated with either Pd or Pt. This behavior was attributed to the absorption of hydrogen by MWCNTs, assisted by the “spill-over” phenomenon due to transition metals decoration, and is stronger for the Pt compound with respect to the Pd one. The TGA measurements performed in isothermal conditions demonstrated that the catalytic efficacy of both the metal decorated MWCNTs was superior to that of pure MWCNTs being (the hydrogen desorption rate was about two-fold higher in the former systems than in the latter one).

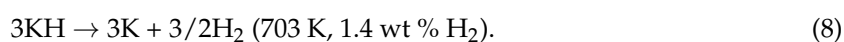
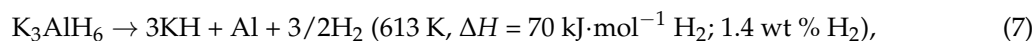
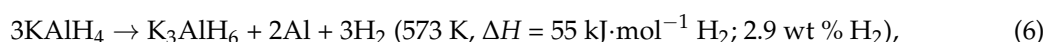
### 2.3. Potassium Alanate $\text{KAlH}_4$

Ashby et al. [15] prepared for the first time potassium alanate by one-step synthesis in toluene, tetrahydrofuran, and diglyme. The last solvent was the optimal one, due to the highest solubility of the alanate in it. Morioka et al. [52] synthesized  $\text{KAlH}_4$  in powder form using KH and Al as reactants under hydrogen pressure >175 bar and temperature of 543 K, as described by Dymova et al. [6], for the preparation of other metal alanates. Hauback et al. [53], according to Bastide et al. [54], prepare K alanate by the addition of  $\text{LiAlH}_4$  to a  $\text{Et}_2\text{O}$  solution of KF and  $\text{AlEt}_3$ , followed by washing the obtained powder with  $\text{Et}_2\text{O}$ . Ares et al. [55], as suggested by Dilts et al. [16], reacted  $\text{AlH}_3$  in diglyme with KH in excess amount obtaining pure K alanate.

$\text{KAlH}_4$  crystallizes in the  $\text{BaSO}_4$  type structure (space group  $Pnma$ ), with  $a = 9.009 \text{ \AA}$ ,  $b = 5.767 \text{ \AA}$ , and  $c = 7.399 \text{ \AA}$  at 0 K, as described by Vajeeston et al. [56], using density functional theory (DFT).

Neutron diffraction experiments at 8 K and 295 K [55] allowed for finding a more detailed structure of the compound; the structure is based on isolated  $\text{AlD}_4^-$  tetrahedra. Every K atom is surrounded by 10 D atoms from seven different  $\text{AlD}_4^-$  groups. The Al–D bond length is 1.589–1.659 Å at 8 K and 1.546–1.669 Å at 295 K, and the bond angles are comprised between 106.4° and 113.3° at 8 K and between 106.2° and 114.6° at 295 K, testifying that the tetrahedral distortion becomes lower by lowering the temperature.

Concerning the hydrogen absorption and desorption properties, this alanate was only scarcely studied. Morioka et al. [52], by temperature programmed desorption (TPD) analyses, proposed the following dehydrogenation mechanism:



These reactions were demonstrated reversible without catalysts addition at relatively low hydrogen pressure and temperatures. The addition of  $\text{TiCl}_3$  was found to decrease the working temperature of the first dehydrogenation step (6) of 50 K [55], but no variations were recorded for the other two reaction steps (7)–(8).

### 2.4. Magnesium Alanate $\text{Mg}(\text{AlH}_4)_2$

Many different synthetic methods were proposed to obtain Mg alanate, starting from Mg hydride and Al chloride or Al hydride in diethyl ether, or from Mg or Mg chloride and Na alanate in THF [57–61]. In any case, not one of them was able to give the pure compound.

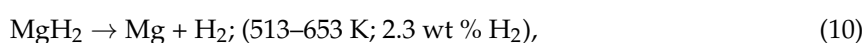
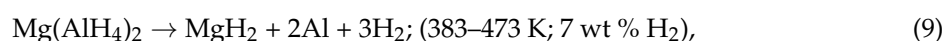
Fichtner and Fuhr synthesized the compound [62] by metathesis reaction between  $\text{NaAlH}_4$  and  $\text{MgCl}_2$  and subsequent Soxhlet extraction, obtaining the solvent adduct  $\text{Mg}(\text{AlH}_4)_2$  with a yield of

81.5%. By solvent evaporation, the alanate (95% purity) was obtained. This successful procedure was followed in many works starting from that point (2002).

Dymova et al. [63] ball milled Mg hydride and Al chloride, obtaining a  $\text{Mg}(\text{AlH}_4)_2\text{-MgCl}_2$  mixture. Recently, Mamatha et al. [64] obtained a mixture of Mg alanate and NaCl by ball milling Na alanate and Mg chloride. Again, the alanate was not obtained alone in a pure form.

Fossdal et al., by X-ray and neutron powder diffraction [65], and by synchrotron radiation experiments [66], found that the crystal structure of  $\text{Mg}(\text{AlH}_4)_2$  is trigonal with space group  $P3m1$ . The tetrahedral  $\text{AlH}_4^-$  groups are coordinated to Mg atoms in a distorted octahedral geometry, giving a sheet-like structure along the crystallographic  $c$ -axis. For this compound, increasing the temperature results in a decrease of the  $\text{AlH}_4^-$  tetrahedral distortion.

The dehydrogenation/decomposition of the Mg alanate takes place by three subsequent steps, which, at the end, produces the intermetallic compound  $\text{Al}_3\text{Mg}_2$ , Al in excess and 9.3 wt % hydrogen [67]:



The total dehydrogenation enthalpy is  $41 \text{ kJ}\cdot\text{mol}^{-1} \text{ H}_2$ , being the first step exothermic and the last ones endothermic. The addition of Ti led to better hydrogen absorption kinetics and reasonable desorption rate at 423 K, but reversibility was not attained under the studied working conditions [68]. Liu et al. [69] prepared Mg alanate submicron rods with 96.1% purity and, analyzing the obtained material by TPD and DSC techniques, found that the first dehydrogenation step evolved through a diffusion-controlled kinetic mechanism with an apparent activation energy of about  $123.0 \text{ kJ}\cdot\text{mol}^{-1}$ . Unfortunately, the amount of hydrogen recharged in the temperature range 413–483 K and at 100 bar of hydrogen pressure was only 2.3 wt %. Several attempts have been made from this work on in order to improve the kinetics of the processes and to make them reversible, but this was not possible because of thermodynamic constraints [70–72].

### 2.5. Calcium Alanate $\text{Ca}(\text{AlH}_4)_2$

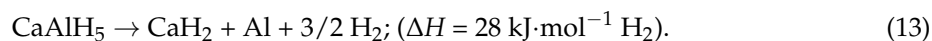
In the 1950s, Schwab and Wintersberger [73] prepared  $\text{Ca}(\text{AlH}_4)_2$  for the first time in the literature, starting from Ca hydride and Al chloride in THF, but the yield was only about 40%. An even lower yield was obtained [74] performing the same reaction in dimethyl ether.

Recently [62,64,75], the solvent adduct  $\text{Ca}(\text{AlH}_4)_2 \cdot x(\text{solvent})$  was prepared under inert atmosphere by wet chemistry. By heating up to moderate temperature under vacuum, the solvent is forced to evaporate, leaving almost pure calcium alanate. Mechanochemical synthesis was also proposed, but the compound has been never obtained in a pure form [75,76].

According to Fichtner [77], the crystal structure of  $\text{Ca}(\text{AlH}_4)_2 \cdot 4\text{THF}$  is monoclinic, space group  $P2_1/m$ , and two formula units are present for unit cell. A molecular structure similar to the analogous Mg alanate was found [67,78], with the calcium ion occupying a crystallographic inversion center octahedrally coordinated by two hydrogen atoms of two  $[\text{AlH}_4]^-$  groups and four oxygen atoms from four solvent molecules.

Lovvik [79], by DFT calculations, found that the  $Pbca$  crystal structure based on  $\text{CaB}_2\text{F}_8$  is as stable as is possible for the pure solvent free alanate. In this arrangement, hydrogen atoms are coordinated around Al atoms in slightly distorted tetrahedrons. The Al–H bond lengths are between 161 and 163 pm and the H–Al–H angles are between  $106.8^\circ$  and  $113.2^\circ$ . Ca atoms are eight coordinated to hydrogen atoms forming distorted square antiprisms, with each corner shared by an  $\text{AlH}_4$  tetrahedron. Using a higher number of input structures, Wolverton and Ozolins confirmed these same findings [17].

The decomposition of  $\text{Ca}(\text{AlH}_4)_2$  takes place in two steps, releasing 5.9 wt %  $\text{H}_2$ , according to the following reactions [80,81]:



The full decomposition of Ca alanate will require the dehydrogenation of  $\text{CaH}_2$  formed in reaction (13); this process is strongly endothermic, with an enthalpy of  $+172 \text{ kJ}\cdot\text{mol}^{-1} \text{H}_2$ , and could take place only at temperatures too high for practical storage applications. The addition of Al to  $\text{CaH}_2$  reduces the dehydrogenation enthalpy of the compound to  $+72 \text{ kJ}\cdot\text{mol}^{-1} \text{H}_2$ , leading to the formation of the intermetallic compound  $\text{CaAl}_2$  [80]. Recently, Iosub et al. [82] described a different decomposition mechanism by DSC analyses: in the calorimetric profile, they obtained three peaks and attributed the first one, exothermic, to reaction (12); the second one, endothermic, to the formation of the intermediate  $\text{Ca}_3(\text{AlH}_6)_2$  from  $\text{CaAlH}_5$  and Al; and the third peak, also endothermic, to the formation of  $\text{CaH}_2$  and Al, with hydrogen release, that is, the same products of reaction (13).

## 2.6. Strontium Alanate $\text{Sr}(\text{AlH}_4)_2$

In 2000, Dymova et al. [83] reported the synthesis of  $\text{Sr}(\text{AlH}_4)_2$  by mechanochemical activation starting from crystals of  $\text{SrH}_2$  and  $\text{AlH}_3$ . The decomposition of the alanate was followed by spectroscopic methods, evidence of the formation of the compound  $\text{SrAlH}_5$  and the aluminium hydride  $\text{AlH}_3$ . In 2012, Pommerin et al. [84] prepared the compound by the metathesis reaction of  $\text{NaAlH}_4$  and  $\text{SrCl}_2$  in a molar ratio of 1.8:1 (with an excess of  $\text{SrCl}_2$ ). The powders were milled by a planetary mill in stainless steel vials at 600 rpm with a balls to powders ratio of about 13:1 for a total time of 9 h (after each 2 h period, the milling vial was transferred into a glovebox, and the powder was homogenized). The reaction led to the formation of the alanate phase together with NaCl. The crystal structure of the alanate, solved from powder X-ray diffraction (XRD) data in combination with solid-state  $^{27}\text{Al}$  nuclear magnetic resonance (NMR) spectroscopy, is orthorhombic (space group  $Pmmm$ ); built up of isolated  $[\text{AlH}_4]^-$  tetrahedra; and the cell parameters are  $a = 9.1165(18) \text{ \AA}$ ,  $b = 5.2164(11) \text{ \AA}$ , and  $c = 4.3346(8) \text{ \AA}$ , respectively.

The calorimetric trace of  $\text{Sr}(\text{AlH}_4)_2$  shows a main exothermic reaction at about 403 K and two endothermic reactions starting above 513 K. During thermolysis, the sample released the first 0.8 wt % hydrogen up to about 393 K, and 1.3 wt % hydrogen in a second step going on up to 573 K.

After rehydrogenation, performed at 300 bar for 3 h, a second dehydrogenation was attempted, accounting for only 0.6 wt %  $\text{H}_2$  release. The diffraction patterns acquired during gradual dehydrogenation of the alanate showed the formation of  $\text{SrAlH}_5$  and then its decomposition, leading to Al in crystalline form and a probable amorphous Sr-containing phase.

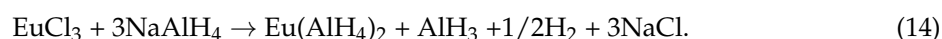
## 2.7. Yttrium Alanate $\text{Y}(\text{AlH}_4)_3$

Transition metal alanates such as Ti and Fe compounds have high theoretical gravimetric capacity (9.3 and 5.8 wt %  $\text{H}_2$ , respectively), but attracted little interest as they were considered thermodynamically unstable. Their synthesis, like that of other compounds such as V, Co, Mn, Cu, Zr, Nb, Ag, Ce, and Ta alanates, was carried out at temperatures between 133 K and 193 K because their decomposition, with hydrogen release, was reported to start in most cases at 223 K or below [85]. Rare earth alanates  $[\text{RE}(\text{AlH}_4)_3]$  (RE = La, Ce, Pr) already start to evolve hydrogen forming  $\text{REAlH}_6$  and Al during ball milling of rare earth chlorides and sodium aluminum hydride [86]. On the contrary,  $\text{Y}(\text{AlH}_4)_3$ , with a theoretical gravimetric capacity of 6.6 wt %  $\text{H}_2$ , was reported to be a little less unstable, starting to decompose from 323 K [87]. In 2017, Cao et al. [88] systematically studied the hydrogen storage properties and the reversibility of the compound prepared by the mechanochemical reaction of  $\text{LiAlH}_4$  and  $\text{YCl}_3$  in a stoichiometric ratio of 3:1. Upon heating, this compound decomposes via a four-stage dehydrogenation process. In particular, in the range 353–443 K,  $\text{YAlH}_6$ , Al, and  $\text{H}_2$  are

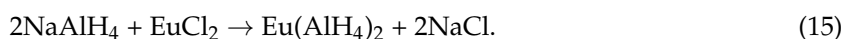
obtained. Increasing the temperature up to 523 K,  $YAlH_6$  decomposes to form  $YH_3$  and additional Al. Further increasing the temperature up to 573 K,  $YH_3$  yields  $YH_2$  and  $H_2$ . Finally, at 623 K, the newly formed  $YH_2$  starts to react with Al to generate  $YAl_3$ . The first step, with a hydrogen release of 3.4 wt % within 60 min at 413 K, is 75% reversible under 100 bar hydrogen pressure, with an apparent activation energy of  $92.1 \text{ kJ}\cdot\text{mol}^{-1}$ ; this is the first time that a transition metal alanate is reported to reversibly absorb hydrogen.

### 2.8. Eu Alanate

In 2009, C. Weidenthaler et al. proved that rare earth aluminium hydrides (La, Ce, Pr compounds), beyond the known ones of the alkaline earth and alkali elements, can be prepared by mechanochemical methods [86]. Motivated by the successful preparation of these compounds, in 2012, the authors studied, for the first time in the literature, europium aluminum hydrides [84]. The complex aluminum hydrides were prepared by the metathesis reaction of  $EuCl_2$  or  $EuCl_3$  with sodium aluminum hydride  $NaAlH_4$ . In a typical experiment, stoichiometric amounts of the corresponding metal chloride and  $NaAlH_4$  were mixed in a glovebox and subsequently milled by a planetary mill in a hardened stainless steel vial at a rotational speed of 500 rpm with a ball to powders ratio of about 40:1 under a hydrogen pressure of 1–15 bar. Milling times were varied between several minutes up to 7 h to ensure an almost complete reaction. The obtaining of the alanate starting from  $EuCl_3$  went through the formation of an unstable product with composition  $[EuCl_2(AlH_4)]$ , which decomposes to  $EuCl_2$  and  $AlH_3$ , and hydrogen release. The formed  $EuCl_2$  further reacts with  $NaCl$  and  $EuCl_3$ , producing the mixed-valent compound  $NaEu_2Cl_6$ , which undergoes a further metathesis reaction with sodium alanate leading to the observed  $Eu(AlH_4)_2$  phase. The overall reaction is as follows:



The formation of the alanate starting from  $EuCl_2$  proceeds via the direct reaction without aluminum hydride formation and hydrogen release.



The crystal structure of the alanate, solved from powder XRD data in combination with solid-state  $^{27}\text{Al}$  NMR spectroscopy, is orthorhombic (space group  $Pmmn$ ) and built up of isolated  $[AlH_4]^-$  tetrahedra. The cell parameters are  $a = 9.1003(13) \text{ \AA}$ ,  $b = 5.1912(8) \text{ \AA}$ , and  $c = 4.2741(5) \text{ \AA}$ , respectively.

For both the starting chlorides mixtures, DSC analyses showed an exothermic peak at about 373 K followed by an endothermic reaction, starting at about 453 K (measurements performed under Ar at 10 K/min) and characterized by hydrogen release. The decomposition enthalpies calculated from the DSC data were  $-4.4 \text{ kJ}\cdot\text{mol}^{-1}$  of  $H_2$  for the first reaction step and  $57 \text{ kJ}\cdot\text{mol}^{-1}$  of  $H_2$  for the second step. Moreover, for the mixture containing  $EuCl_3$ , an additional endothermic reaction with an onset at about 353 K was observed. This event was correlated to the decomposition of  $AlH_3$ . The dehydrogenation of the mixtures obtained from  $EuCl_2$  and  $EuCl_3$  proceeded in two steps, with the first stage releasing 0.6 wt %  $H_2$  and 0.8 wt % and the second step about 1.1 wt %  $H_2$  and 1.0 wt %, respectively. After rehydrogenation, performed at 300 bar for 3 h, a second dehydrogenation was performed, accounting for only 0.7 wt %  $H_2$  and 0.8 wt %  $H_2$  release. The scarce reversibility under quite mild conditions could be due to the exothermal character of the first dehydrogenation step. X-ray powder diffraction analyses performed at room temperature on samples heated up to increase temperature from 373 K to 873 K showed that the alanate dehydrogenated leads to the formation of  $EuAlH_5$ , which, in turn, decomposed forming the intermetallic compound  $EuAl_4$ . Its partial rehydrogenation led to the formation of  $EuH_x$  phases, without traces of the desired alanate. The amount of re-absorbed hydrogen is by far too low to consider Eu alanate as potential solid-state hydrogen-storage material.

### 2.9. Multi-Cation Alanates

All the alkali alanates discussed above are unsuitable for practical applications because of kinetic and/or thermodynamic limitations. These shortcomings led researchers to try synthesizing and testing some multi-cation alanates, that is, alanates containing more than one alkaline or alkaline earth metal, as hydrogen absorbing materials.

Claudy prepared the Na–Li alanate (i.e.,  $\text{Na}_2\text{LiAlH}_6$ ) [89] by reacting  $\text{LiAlH}_4$  with  $\text{NaH}$  either in toluene solution or by a solid-state reaction at both high temperature and hydrogen pressure. Concerning the mechanochemical synthesis, Huot et al. prepared the compound [90] by ball milling a mixture of  $\text{NaH}$ ,  $\text{LiH}$ , and  $\text{NaAlH}_4$  for 40 h, while Brinks et al. [91] ball milled  $\text{LiAlD}_4$  and  $2\text{NaAlD}_4$  and then annealed the powder mixture under 30 bar  $\text{D}_2$  pressure at 453 K. The crystal structure of the compound is an ordered double perovskite-type structure with Li and Al in octahedral positions. These results, obtained by X-ray and neutron diffraction, are consistent with the DFT calculations performed by Lovvik et al. [92]. Graetz et al. [93] performed several pressure-composition-isotherm measurements on pristine and catalysed  $\text{Na}_2\text{LiAlH}_6$  at different temperatures, finding an initial hydrogen storage capacity of 3.2 and 3.0 wt %, respectively, which reduces down to 2.8 and 2.6 wt % in the subsequent cycles. By these experiments, through the van't Hoff plot, a dehydrogenation enthalpy of  $53.5 \pm 1.2 \text{ kJ}\cdot\text{mol}^{-1} \text{ H}_2$  was found.

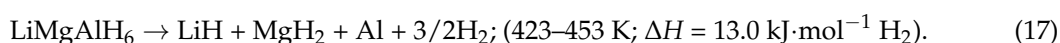
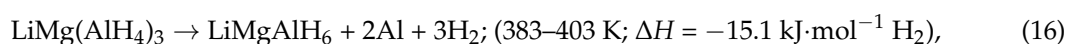
The K–Na alanate was prepared by Sorby et al. [94], starting from a mixture of  $\text{KH}$  and  $\text{NaAlH}_4$  that was first ball milled and then annealed for 18 h at 423 K under a hydrogen pressure of 100 bar.

A cubic ordered perovskite-type structure with space group  $Fm-3m$  ( $a = 8.118 \text{ \AA}$ ) was determined for the compound by X-ray and neutron powder diffraction. In this structure, the hydrogen atoms point towards the octahedral interstices of the close packed  $\text{AlH}_6^{3-}$  units, all filled with  $\text{K}^+$  ions coordinated with respect to hydrogen.  $\text{K}_2\text{NaAlH}_6$  dehydrogenates at  $\sim 625 \text{ K}$  under low hydrogen pressure and reveals appreciable re-hydrogenation kinetics under 6 bar hydrogen pressure at 573 K [95]. Graphene sheet and single wall carbon nanotube SWCNT were tested as additives for  $\text{K}_2\text{NaAlH}_6$ ; a destabilizing activity was found, with the hydrogen desorption temperature decreasing down to  $\sim 620 \text{ K}$  and  $\sim 615 \text{ K}$ , respectively. Halides was also revealed to be more active; in particular,  $\text{TiF}_3$  was found to be both a good catalyst and an efficient destabilizing agent. Because of its presence, the desorption temperature of the alanate decreased from 625 K to 598 K and the desorption activation energy reduced from  $124.43 \text{ kJ}\cdot\text{mol}^{-1}$  to  $88.05 \text{ kJ}\cdot\text{mol}^{-1}$ . The amount of hydrogen released is about 2.8 wt % [93], but the process was not fully reversible.

Ball milling  $\text{LiAlH}_4$  and  $\text{KH}$  in a 1:2 molar ratio and heating the obtained mixture up to 593–603 K under 100–700 bar for 1–2 days produces K–Li alanate  $\text{K}_2\text{LiAlH}_6$  [96], whose crystal structure [93] is cubic ( $Fm-3m$ ). DFT calculations confirmed this finding and outlined the similarity with the face centered cubic low temperature phase  $\text{K}_2\text{LiAlF}_6$  [92]. More recently [96], a rhombohedral-type structure with space group  $R3m$  was proposed for the compound, where cation mixing was excluded by Rietveld analysis. To the authors knowledge, the hydrogenation and dehydrogenation properties of this compound have not been characterized yet.

$\text{LiMg}(\text{AlD}_4)_3$  was first synthesized by Bulychev et al. in 1979 from  $\text{LiAlH}_4$ ,  $\text{NaAlH}_4$ , and  $\text{MgCl}_2$  in ether [97]. Recently, Mamatha et al. [65,83] prepared ball milled  $\text{LiAlH}_4$  and  $\text{MgCl}_2$  in a molar ratio of 3:1, and obtained the mixed Li–Mg compound with  $\text{LiCl}$  as a by-product. Its crystal structure is monoclinic,  $P_{21}/c$  space group, and consists of a corner sharing network of alternating  $\text{AlD}_4$  tetrahedrons and  $\text{LiD}_6$  or  $\text{MgD}_6$  octahedrons [98,99].

The compound dehydrogenates in the two following steps:



It is not suitable for practical applications, as is the case for all the alanates described above, because of thermodynamic limitations [100].

### 2.10. Reactive Hydrides Composites

In the attempt to improve the hydrogen absorption and desorption properties of the alanates and to make their characteristics as close as possible to practical applications, these compounds were also combined with other hydrides in the reactive hydrides composites (RHC) strategy. For example, Mohtadi et al. [101] prepared the  $\text{NaAlH}_4 + \text{LiBH}_4$  and the  $\text{LiAlH}_4 + \text{LiBH}_4 + \text{CaCl}_2$  systems. Metathesis exchange reactions were observed for the first RHC, resulting in the formation of  $\text{LiAlH}_4$  and  $\text{NaBH}_4$ . In any case, no interaction was observed between the two hydrides, and the decomposition steps of the alanate took place as for the pure compound.

On the other hand, for the  $\text{LiAlH}_4 + \text{LiBH}_4 + \text{CaCl}_2$  system, a calcium alanate-type phase formed, with a different local coordination geometry of the  $\text{AlH}_4^-$  anions with respect to the structure observed in pure calcium alanate. This difference was attributed to interactions between the  $[\text{AlH}_4]^-$  groups and the  $[\text{BH}_4]^-$  anions. The dehydrogenation of the system took place in the temperature range of 403–473 K, with a hydrogen release amount of 2.3 wt %.

The  $\text{MgH}_2\text{-NaAlH}_4$  composite system was found to have improved dehydrogenation properties with respect to the pristine as-milled  $\text{NaAlH}_4$  and  $\text{MgH}_2$  compounds [102], probably due to the formation of the  $\text{NaMgH}_3$  and  $\text{Mg}_{17}\text{Al}_{12}$  phases during the dehydrogenation process.

Shi et al. [103] and Ravensbaek et al. [104] studied the  $\text{LiBH}_4\text{-NaAlH}_4$  system and claimed a conversion to  $\text{LiAlH}_4\text{-NaBH}_4$  and a mutual destabilization between the alanate and the borohydride phases.

Subsequently, Ismail [105] prepared the ternary  $\text{NaAlH}_4\text{-MgH}_2\text{-LiBH}_4$  (1:1:1) system by ball milling and showed its superior hydrogen storage properties with respect to the unary components. Ball milling activated the conversion from the starting mixture to a  $\text{LiAlH}_4\text{-MgH}_2\text{-NaBH}_4$  system. Considering dehydrogenation, below 523 K,  $\text{LiAlH}_4$  decomposed into  $\text{LiH}$  and  $\text{Al}$  with hydrogen release. At 523 K and 623 K,  $\text{LiH}$  and  $\text{Al}$  reacted with  $\text{MgH}_2$  to produce and  $\text{Li}_3\text{Mg}$ ,  $\text{Mg}_{17}\text{Al}_{12}$ , and  $\text{Mg}_2\text{Al}_3$ , with hydrogen release. With a further temperature increase to 748 K, the reaction between  $\text{NaBH}_4$  and  $\text{Mg}_{17}\text{Al}_{12}$  took place, yielding  $\text{NaH}$  and  $\text{Mg}_{1-x}\text{Al}_xB_2$ , and full hydrogen release. DSC measurements indicated that the enthalpy change in the second and third decomposition steps are 61 and 100  $\text{kJ}\cdot\text{mol}^{-1} \text{H}_2$ , respectively. Those values are smaller than that of  $\text{MgH}_2$  and  $\text{NaBH}_4$  alone (76 and 191  $\text{kJ}\cdot\text{mol}^{-1} \text{H}_2$ ). The Kissinger plots for different heating rates in DSC show that the apparent activation energy,  $E_A$ , for the decomposition of  $\text{MgH}_2$  and  $\text{NaBH}_4$  is reduced to 96.85 and 111.74  $\text{kJ}\cdot\text{mol}^{-1}$ , respectively. The formation of intermediate  $\text{Li-Mg}$ ,  $\text{Mg-Al}$ , and  $\text{Mg-Al-B}$  alloys upon dehydrogenation alters the de/rehydrogenation pathway, leading to favorable variations in the thermodynamic parameters with respect to the pristine compounds. The same consideration can be applied to the ternary  $\text{LiAlH}_4\text{-MgH}_2\text{-LiBH}_4$  system [12], which also exhibits superior hydrogen storage properties compared with the pristine hydrides ( $\text{LiAlH}_4$ ,  $\text{MgH}_2$ , and  $\text{LiBH}_4$ ).

Nakagawa et al. [13], after the interesting preliminary works reported in the literature [106,107] regarding the interactions between some alanates and ammonia borane, studied the hydrogen desorption properties and decomposition processes of  $\text{NH}_3\text{BH}_3\text{-MAlH}_4$  ( $M = \text{Na, Li}$ ) composites. They obtained a hydrogen desorption release up to 5 wt % below 533 K due to three exothermic reactions, without release of  $\text{NH}_3$ ,  $\text{B}_2\text{H}_6$ , and  $\text{B}_3\text{H}_6\text{N}_3$ . In particular, the first reaction was ascribed to the formation of the mixed-metal amidoborane phase, the second to the decomposition of mixed-metal amidoborane, while the third step is a combination of different reactions; that is, the reaction between  $\text{AB}$  and  $\text{MAlH}_4$  ( $M = \text{Na, Li}$ ), which results in the formation of  $\text{MBH}_4$ , and the reaction between  $\text{M}_3\text{AlH}_6$  ( $M = \text{Na, Li}$ ) and  $\text{AB}$ , which gives another mixed-metal amidoborane. The obtained results underline the importance of the mixed phases as a barrier against by-product gas emission in the amino-borane based systems.

### 3. Conclusions

In this review, the most relevant materials studied in the last 20 years concerning solid-state hydrogen storage in the family of alanates are described. We reported their structural and physico-chemical properties and the thermodynamic and kinetics features of their hydrogen

absorption and desorption mechanisms, and we outlined both their advantages and their drawbacks. The presented results show that the alanates systems are quite interesting concerning their total hydrogen content, but unfortunately for some of them, the dehydrogenated products cannot be rehydrogenated under conditions reasonable for practical applications, and for some others, the last desorption step takes place at temperatures too high for practical applications. The reduced storage capacity obtained considering only the first two steps could be promising for stationary applications, if kinetics limitations are overcome. In this respect, encapsulations and reactive hydride composites strategies could be very appealing. Currently, doped  $\text{NaAlH}_4$ —the system that started the “alanate story” in the late 1990s with Bogdanovic and co-workers [3]—with a decomposition temperature near the working temperature of a proton-exchange membrane fuel cell, is still the most promising—and hence, the most studied—material for achieving practical mobile use in the short term [108]. In any case, the research performed up to now on alanates and described here is a very good starting point for introducing them as possible materials for electrochemical applications, opening new perspectives for the complex hydrides systems utilizations [109].

**Author Contributions:** C.M. conceived the design of the structure of the work together with C.P. and S.G., F.G. and A.M. also contributed with the writing and correction of the paper. T.K. and M.D. contributed with the correction of the paper.

**Conflicts of Interest:** The authors declare no conflict of interest.

## References

1. Mohatadi, R.; Orimo, S. The renaissance of hydrides as energy materials. *Nat. Rev. Mater.* **2016**, *2*. [[CrossRef](#)]
2. He, T.; Pachfule, P.; Wu, H.; Xu, Q.; Chen, P. Hydrogen carriers. *Nat. Rev. Mater.* **2016**, *1*, 16059. [[CrossRef](#)]
3. Bogdanovic, B.; Schwickardi, M. Ti-doped alkali metal aluminium hydrides as potential novel reversible hydrogen storage materials. *J. Alloys Compd.* **1997**, *253–254*. [[CrossRef](#)]
4. Ashby, E.; Brendel, G.; Redman, H. Direct synthesis of complex metal hydrides. *Inorg. Chem.* **1963**, *2*, 499–504. [[CrossRef](#)]
5. Clasen, H. Alanat Synthese aus den Elementen und ihre Bedeutung. *Angew. Chem.* **1961**, *73*, 322–331. [[CrossRef](#)]
6. Dymova, T.; Eliseeva, N.; Bakum, S.; Dergachev, Y. Direct synthesis of alkali metal tetrahydroaluminates in melts. *Dokl. Akad. Nauk. SSSR* **1974**, *125*, 1369.
7. Zaluska, A.; Zaluski, L.; Ström-Olsen, J. Structure, catalysis and atomic reactions on the nano-scale: A systematic approach to metal hydrides for hydrogen storage. *Appl. Phys. A* **2001**, *72*, 157–165. [[CrossRef](#)]
8. Von Colbe, J.M.B.; Felderhoff, M.; Bogdanovic, B.; Schuth, F.; Weidenthaler, C. One-step direct synthesis of a Ti-doped sodium alanate hydrogen storage material. *Chem. Commun.* **2005**, *37*, 4732–4734. [[CrossRef](#)] [[PubMed](#)]
9. Lauher, J.; Dougherty, D.; Herley, P. Sodium tetrahydroaluminate. *Acta Crystallogr. Sect. B Struct. Crystallogr. Cryst. Chem.* **1979**, *35*, 1454–1456. [[CrossRef](#)]
10. Hauback, B.; Brinks, H.; Jensen, C.; Murphy, K.; Maeland, A. Neutron diffraction structure determination of  $\text{NaAlD}_4$ . *J. Alloys Compd.* **2003**, *358*, 142–145. [[CrossRef](#)]
11. Bogdanović, B.; Eberle, U.; Felderhoff, M.; Schüth, F. Complex aluminum hydrides. *Scr. Mater.* **2007**, *56*, 813–816. [[CrossRef](#)]
12. Mao, J.; Guo, Z.; Leng, H.; Wu, Z.; Guo, Y.; Yu, X.; Liu, H. Reversible hydrogen storage in destabilized  $\text{LiAlH}_4$ - $\text{MgH}_2$ - $\text{LiBH}_4$  ternary-hydride system doped with  $\text{TiF}_3$ . *J. Phys. Chem. C* **2010**, *26*, 11643–11649. [[CrossRef](#)]
13. Nakagawa, Y.; Ikarashi, Y.; Isobe, S.; Hino, S.; Ohnuki, S. Ammonia borane–metal alanate composites: Hydrogen desorption properties and decomposition processes. *RSC Adv.* **2014**, *4*, 20626–20631. [[CrossRef](#)]
14. Bogdanović, B.; Sandrock, G. Catalyzed complex metal hydrides. *MRS Bull.* **2002**, *27*, 712–716. [[CrossRef](#)]
15. Ashby, E.; Kobetz, P. The direct synthesis of  $\text{Na}_3\text{AlH}_6$ . *Inorg. Chem.* **1966**, *5*, 1615–1617. [[CrossRef](#)]
16. Dilts, J.; Ashby, E. Thermal decomposition of complex metal hydrides. *Inorg. Chem.* **1972**, *11*, 1230–1236. [[CrossRef](#)]

17. Wolverton, C.; Ozoliņš, V. Hydrogen storage in calcium alanate: First-principles thermodynamics and crystal structures. *Phys. Rev. B* **2007**, *75*, 064101. [[CrossRef](#)]
18. Zidan, R.A.; Takara, S.; Hee, A.G.; Jensen, C.M. Hydrogen cycling behavior of zirconium and titanium–zirconium-doped sodium aluminum hydride. *J. Alloys Compd.* **1999**, *285*, 119–122. [[CrossRef](#)]
19. Wang, J.; Ebner, A.; Zidan, R.; Ritter, J. Synergistic effects of co-dopants on the dehydrogenation kinetics of sodium aluminum hydride. *J. Alloys Compd.* **2005**, *391*, 245–255. [[CrossRef](#)]
20. Lee, G.-J.; Kim, J.W.; Shim, J.-H.; Cho, Y.W.; Lee, K.S. Synthesis of ultrafine titanium aluminide powders and their catalytic enhancement in dehydrogenation kinetics of NaAlH<sub>4</sub>. *Scr. Mater.* **2007**, *56*, 125–128. [[CrossRef](#)]
21. Zaluska, A.; Zaluski, L.; Ström-Olsen, J. Sodium alanates for reversible hydrogen storage. *J. Alloys Compd.* **2000**, *298*, 125–134. [[CrossRef](#)]
22. Pukazhselvan, D.; Gupta, B.K.; Srivastava, A.; Srivastava, O.N. Investigations on hydrogen storage behavior of CNT doped NaAlH<sub>4</sub>. *J. Alloys Compd.* **2005**, *403*, 312–317. [[CrossRef](#)]
23. Berseth, P.A.; Harter, A.G.; Zidan, R.; Blomqvist, A.; Araújo, C.M.; Scheicher, R.H.; Ahuja, R.; Jena, P. Carbon nanomaterials as catalysts for hydrogen uptake and release in NaAlH<sub>4</sub>. *Nano Lett.* **2009**, *9*, 1501–1505. [[CrossRef](#)] [[PubMed](#)]
24. Atakli, Z.Ö.K.; Callini, E.; Kato, S.; Mauron, P.; Orimo, S.-I.; Züttel, A. The catalyzed hydrogen sorption mechanism in alkali alanates. *Phys. Chem. Chem. Phys.* **2005**, *17*, 20932–20940. [[CrossRef](#)] [[PubMed](#)]
25. Zaluski, L.; Zaluska, A.; Ström-Olsen, J. Hydrogenation properties of complex alkali metal hydrides fabricated by mechano-chemical synthesis. *J. Alloys Compd.* **1999**, *290*, 71–78. [[CrossRef](#)]
26. Baldé, C.P.; Hereijgers, B.P.; Bitter, J.H.; Jong, K.P.D. Sodium Alanate Nanoparticles—Linking Size to Hydrogen Storage Properties. *J. Am. Chem. Soc.* **2008**, *130*, 6761–6765. [[CrossRef](#)] [[PubMed](#)]
27. Fichtner, M.; Engel, J.; Fuhr, O.; Glöss, A.; Rubner, O.; Ahlrichs, R. The structure of magnesium alanate. *Inorg. Chem.* **2003**, *42*, 7060–7066. [[CrossRef](#)] [[PubMed](#)]
28. Graetz, J.; Wegrzyn, J.; Reilly, J.J. Regeneration of lithium aluminum hydride. *J. Am. Chem. Soc.* **2008**, *130*, 17790–17794. [[CrossRef](#)] [[PubMed](#)]
29. Wang, J.; Ebner, A.D.; Ritter, J.A. Physicochemical pathway for cyclic dehydrogenation and rehydrogenation of LiAlH<sub>4</sub>. *J. Am. Chem. Soc.* **2006**, *128*, 5949–5954. [[CrossRef](#)] [[PubMed](#)]
30. Kojima, Y.; Kawai, Y.; Haga, T.; Matsumoto, M.; Koiwai, A. Direct formation of LiAlH<sub>4</sub> by a mechanochemical reaction. *J. Alloys Compd.* **2007**, *441*, 189–191. [[CrossRef](#)]
31. Sklar, N.; Post, B. Crystal structure of lithium aluminum hydride. *Inorg. Chem.* **1967**, *6*, 669–671. [[CrossRef](#)]
32. Hauback, B.; Brinks, H.; Fjellvåg, H. Accurate structure of LiAlD<sub>4</sub> studied by combined powder neutron and X-ray diffraction. *J. Alloys Compd.* **2002**, *346*, 184–189. [[CrossRef](#)]
33. Resan, M.; Hampton, M.D.; Lomness, J.K.; Slattery, D.K. Effects of various catalysts on hydrogen release and uptake characteristics of LiAlH<sub>4</sub>. *Int. J. Hydrogen Energy* **2005**, *30*, 1413–1416. [[CrossRef](#)]
34. Ares, J.; Aguey-Zinsou, K.-F.; Porcu, M.; Sykes, J.; Dornheim, M.; Klassen, T.; Bormann, R. Thermal and mechanically activated decomposition of LiAlH<sub>4</sub>. *Mater. Res. Bull.* **2008**, *43*, 1263–1275. [[CrossRef](#)]
35. Balema, V.; Wiench, J.; Dennis, K.; Pruski, M.; Pecharsky, V. Titanium catalyzed solid-state transformations in LiAlH<sub>4</sub> during high-energy ball-milling. *J. Alloys Compd.* **2001**, *329*, 108–114. [[CrossRef](#)]
36. Zhou, S.; Zou, J.; Zeng, X.; Ding, W. Effects of RE<sub>3</sub> (RE = Y, La, Ce) additives on dehydrogenation properties of LiAlH<sub>4</sub>. *Int. J. Hydrogen Energy* **2014**, *39*, 11642–11650. [[CrossRef](#)]
37. Zhai, F.; Li, P.; Sun, A.; Wu, S.; Wan, Q.; Zhang, W.; Li, Y.; Cui, L.; Qu, X. Significantly improved dehydrogenation of LiAlH<sub>4</sub> destabilized by MnFe<sub>2</sub>O<sub>4</sub> nanoparticles. *J. Phys. Chem. C* **2012**, *116*, 11939–11945. [[CrossRef](#)]
38. Rafiud, D.; Zhang, L.; Ping, L.; Qu, X. Catalytic effects of nano-sized TiC additions on the hydrogen storage properties of LiAlH<sub>4</sub>. *J. Alloys Compd.* **2010**, *508*, 119–128. [[CrossRef](#)]
39. Ismail, M.; Zhao, Y.; Yu, X.; Ranjbar, A.; Dou, S. Improved hydrogen desorption in lithium alanate by addition of SWCNT–metallic catalyst composite. *Int. J. Hydrogen Energy* **2011**, *36*, 3593–3599. [[CrossRef](#)]
40. Rafiud, D.; Xuanhui, Q.; Ping, L.; Zhang, L.; Ahmad, M. Hydrogen Sorption Improvement of LiAlH<sub>4</sub> Catalyzed by Nb<sub>2</sub>O<sub>5</sub> and Cr<sub>2</sub>O<sub>3</sub> Nanoparticles. *J. Phys. Chem. C* **2011**, *115*, 13088–13099. [[CrossRef](#)]
41. Ismail, M.; Zhao, Y.; Yu, X.; Dou, S. Effects of NbF<sub>5</sub> addition on the hydrogen storage properties of LiAlH<sub>4</sub>. *Int. J. Hydrogen Energy* **2010**, *35*, 2361–2367. [[CrossRef](#)]
42. Rafiud, D.; Qu, X.; Li, X.; Ahmad, M.; Lin, Z. Comparative catalytic effects of NiCl<sub>2</sub>, TiC and TiN on hydrogen storage properties of LiAlH<sub>4</sub>. *Rare Met.* **2011**, *30*, 27–34. [[CrossRef](#)]

43. Ares Fernandez, J.R.; Aguey-Zinsou, F.; Elsaesser, M.; Ma, X.Z.; Dornheim, M.; Klassen, T.; Bormann, R. Mechanical and thermal decomposition of  $\text{LiAlH}_4$  with metal halides. *Int. J. Hydrogen Energy* **2007**, *32*, 1033–1040. [[CrossRef](#)]
44. Li, Z.; Liu, S.; Si, X.; Zhang, J.; Jiao, C.; Wang, S.; Liu, S.; Zou, Y.-J.; Sun, L.; Xu, F. Significantly improved dehydrogenation of  $\text{LiAlH}_4$  destabilized by  $\text{K}_2\text{TiF}_6$ . *Int. J. Hydrogen Energy* **2012**, *37*, 3261–3267. [[CrossRef](#)]
45. Li, L.; Qiu, F.; Wang, Y.; Xu, Y.; An, C.; Liu, G.; Jiao, L.; Yuan, H. Enhanced hydrogen storage properties of  $\text{TiN-LiAlH}_4$  composite. *Int. J. Hydrogen Energy* **2013**, *38*, 3695–3701. [[CrossRef](#)]
46. Chen, J.; Kuriyama, N.; Xu, Q.; Takeshita, H.T.; Sakai, T. Reversible hydrogen storage via titanium-catalyzed  $\text{LiAlH}_4$  and  $\text{Li}_3\text{AlH}_6$ . *J. Phys. Chem. B* **2001**, *105*, 11214–11220. [[CrossRef](#)]
47. Blanchard, D.; Brinks, H.; Hauback, B.; Norby, P. Desorption of  $\text{LiAlH}_4$  with Ti- and V-based additives. *Mater. Sci. Eng. B* **2004**, *108*, 54–59. [[CrossRef](#)]
48. Zheng, X.; Qu, X.; Humail, I.S.; Li, P.; Wang, G. Effects of various catalysts and heating rates on hydrogen release from lithium alanate. *Int. J. Hydrogen Energy* **2007**, *32*, 1141–1144. [[CrossRef](#)]
49. Kojima, Y.; Kawai, Y.; Matsumoto, M.; Haga, T. Hydrogen release of catalyzed lithium aluminum hydride by a mechanochemical reaction. *J. Alloys Compd.* **2008**, *462*, 275–278. [[CrossRef](#)]
50. Sun, T.; Huang, C.K.; Wang, H.; Sun, L.X.; Zhu, M. The effect of doping  $\text{NiCl}_2$  on the dehydrogenation properties of  $\text{LiAlH}_4$ . *Int. J. Hydrogen Energy* **2008**, *33*, 6216–6221. [[CrossRef](#)]
51. Tan, C.-Y.; Tsai, W.-T. Catalytic and inhibitive effects of Pd and Pt decorated MWCNTs on the dehydrogenation behavior of  $\text{LiAlH}_4$ . *Int. J. Hydrogen Energy* **2015**, *40*, 10185–10193. [[CrossRef](#)]
52. Morioka, H.; Kakizaki, K.; Chung, S.-C.; Yamada, A. Reversible hydrogen decomposition of  $\text{KAlH}_4$ . *J. Alloys Compd.* **2003**, *353*, 310–314. [[CrossRef](#)]
53. Hauback, J.; Brinks, H.; Heyn, R.; Blom, R.; Fjellvåg, H. The crystal structure of  $\text{KAlD}_4$ . *J. Alloys Compd.* **2005**, *394*, 35–38. [[CrossRef](#)]
54. Bastide, J.; El Hajri, J.; Claudy, P.; El Hajbi, A. A New Route to Alkali Metal Aluminum Hydrides  $\text{MAlH}_4$  with  $\text{M} = \text{Na, K, Rb, Cs}$  and Structural Features for the Whole Family with  $\text{M} = \text{Li to Cs}$ . *Synth. React. Inorg. Met.-Org. Chem.* **1995**, *25*, 1037–1047. [[CrossRef](#)]
55. Ares, J.R.; Aguey-Zinsou, K.-F.; Leardini, F.; Ferrer, I.J.; Fernandez, J.-F.; Guo, Z.-X.; Sánchez, C. Hydrogen absorption/desorption mechanism in potassium alanate ( $\text{KAlH}_4$ ) and enhancement by  $\text{TiCl}_3$  doping. *J. Phys. Chem. C* **2009**, *113*, 6845–6851. [[CrossRef](#)]
56. Vajeeston, P.; Ravindran, P.; Kjekshus, A.; Fjellvåg, H. Crystal structure of  $\text{KAlH}_4$  from first principle calculations. *J. Alloys Compd.* **2004**, *363*, L8–L12. [[CrossRef](#)]
57. Wiberg, E.; Bauer, R. Magnesium aluminum hydride,  $\text{Mg}(\text{AlH}_4)_2$ . *Z. Naturforsch. B* **1950**, *5*, 397–398.
58. Wiberg, E. Neuere Ergebnisse der präparativen Hydrid-Forschung. *Angew. Chem.* **1953**, *65*, 16. [[CrossRef](#)]
59. Wiberg, E.; Bauer, R. Further studies on  $\text{Mg}(\text{AlH}_4)_2$ . *Z. Naturforsch.* **1952**, *7*, 131.
60. Hertwig, A. Verfahren zur Herstellung Aluminiumhaltiger Hydride. German Patent DE921986, 7 January 1955.
61. Plešek, J.; Hermanek, S. Synthesis and properties of magnesium aluminum hydride. *Collect. Czech. Chem. Commun.* **1966**, *31*, 3060–3067. [[CrossRef](#)]
62. Fichtner, M.; Fuhr, O. Synthesis and structures of magnesium alanate and two solvent adducts. *J. Alloys Compd.* **2002**, *345*, 286–296. [[CrossRef](#)]
63. Dymova, T.; Maltseva, N.; Konoplev, V.; Golovanova, A.; Aleksandrov, D.; Sizareva, A. Solid-phase solvate-free formation of magnesium hydroaluminates  $\text{Mg}(\text{AlH}_4)_2$  and  $\text{MgAlH}_5$  upon mechanochemical activation or heating of magnesium hydride and aluminum chloride mixtures. *Russ. J. Coord. Chem.* **2003**, *29*, 385–389. [[CrossRef](#)]
64. Mamatha, M.; Bogdanović, B.; Felderhoff, M.; Pommerin, A.; Schmidt, W.; Schüth, F.; Weidenthaler, C. Mechanochemical preparation and investigation of properties of magnesium, calcium and lithium–magnesium alanates. *J. Alloys Compd.* **2006**, *407*, 78–86. [[CrossRef](#)]
65. Fossdal, A.; Brinks, H.; Fichtner, M.; Hauback, B. Thermal decomposition of  $\text{Mg}(\text{AlH}_4)_2$  studied by in situ synchrotron X-ray diffraction. *J. Alloys Compd.* **2005**, *404*, 752–756. [[CrossRef](#)]
66. Fossdal, A.; Brinks, H.; Fichtner, M.; Hauback, B. Determination of the crystal structure of  $\text{Mg}(\text{AlH}_4)_2$  by combined X-ray and neutron diffraction. *J. Alloys Compd.* **2005**, *387*, 47–51. [[CrossRef](#)]
67. Fichtner, M.; Fuhr, O.; Kircher, O. Magnesium alanate—A material for reversible hydrogen storage? *J. Alloys Compd.* **2003**, *356*, 418–422. [[CrossRef](#)]

68. Wang, J.; Ebner, A.D.; Ritter, J.A. On the reversibility of hydrogen storage in novel complex hydrides. *Adsorption* **2005**, *11*, 811–816. [[CrossRef](#)]
69. Liu, Y.; Pang, Y.; Zhang, X.; Zhou, Y.; Gao, M.; Pan, H. Synthesis and hydrogen storage thermodynamics and kinetics of Mg(AlH<sub>4</sub>)<sub>2</sub> submicron rods. *Int. J. Hydrogen Energy* **2012**, *37*, 18148–18154. [[CrossRef](#)]
70. Kim, Y.; Lee, F.-K.; Shim, J.H.; Cho, Y.W.; Yoon, K.B. Mechanochemical synthesis and thermal decomposition of Mg(AlH<sub>4</sub>)<sub>2</sub>. *J. Alloys Compd.* **2006**, *422*, 283–287. [[CrossRef](#)]
71. Varin, R.A.; Chiu, C.; Czujko, T.; Wronski, Z. Mechano-chemical activation synthesis (MCAS) of nanocrystalline magnesium alanate hydride [Mg(AlH<sub>4</sub>)<sub>2</sub>] and its hydrogen desorption properties. *J. Alloys Compd.* **2007**, *439*, 302–311. [[CrossRef](#)]
72. Jeong, H.; Kim, T.K.; Choo, K.Y.; Song, I.K. Hydrogen evolution performance of magnesium alanate prepared by a mechanochemical metathesis reaction method. *Korean J. Chem. Eng.* **2008**, *25*, 268. [[CrossRef](#)]
73. Schwab, W.; Wintersberger, K. The preparation and properties of calcium aluminum hydride, Ca(AlH<sub>4</sub>)<sub>2</sub>. *Z. Naturforsch. B* **1953**, *8*, 690.
74. Finholt, A.; Barbaras, G.D.; Barbaras, G.K.; Urry, G.; Wartik, T.; Schlesinger, H. The preparation of sodium and calcium aluminium hydrides. *J. Inorg. Nucl. Chem.* **1955**, *1*, 317–325. [[CrossRef](#)]
75. Maltseva, N.; Golovanova, A.; Dymova, T.; Aleksandrov, D. Solid-phase formation of calcium hydridoaluminates Ca(AlH<sub>4</sub>)<sub>2</sub> and CaHAlH<sub>4</sub> upon mechanochemical activation or heating of mixtures of calcium hydride with aluminum chloride. *Russ. J. Inorg. Chem.* **2001**, *46*, 1793–1797.
76. Schwarz, M.; Haiduc, A.; Stil, H.; Paulus, P.; Geerlings, H. The use of complex metal hydrides as hydrogen storage materials: Synthesis and XRD-studies of Ca(AlH<sub>4</sub>)<sub>2</sub> and Mg(AlH<sub>4</sub>)<sub>2</sub>. *J. Alloys Compd.* **2005**, *404*, 762–765. [[CrossRef](#)]
77. Fichtner, M.; Frommen, C.; Fuhr, O. Synthesis and properties of calcium alanate and two solvent adducts. *Inorg. Chem.* **2005**, *44*, 3479–3484. [[CrossRef](#)] [[PubMed](#)]
78. Nöth, H.; Schmidt, M.; Treit, A. Synthesis and structures of magnesium tetrahydridoaluminates. *Chem. Ber.* **1995**, *128*, 999–1006. [[CrossRef](#)]
79. Løvvik, O. Crystal structure of Ca(AlH<sub>4</sub>)<sub>2</sub> predicted from density-functional band-structure calculations. *Phys. Rev. B* **2005**, *71*, 144111. [[CrossRef](#)]
80. Klaveness, A.; Vajeeston, P.; Ravindran, P.; Fjellvåg, H.; Kjekshus, A. Structure and bonding in BAlH<sub>5</sub> (B = Be, Ca, Sr) from first-principle calculations. *J. Alloys Compd.* **2007**, *433*, 225–232. [[CrossRef](#)]
81. Mamatha, M.; Weidenthaler, C.; Pommerin, A.; Felderhoff, M.; Schüth, F. Comparative studies of the decomposition of alanates followed by in situ XRD and DSC methods. *J. Alloys Compd.* **2006**, *416*, 303–314. [[CrossRef](#)]
82. Iosub, V.; Matsunaga, T.; Tange, K.; Ishikiriyama, M. Direct synthesis of Mg(AlH<sub>4</sub>)<sub>2</sub> and CaAlH<sub>5</sub> crystalline compounds by ball milling and their potential as hydrogen storage materials. *Int. J. Hydrogen Energy* **2009**, *34*, 906–912. [[CrossRef](#)]
83. Dymova, T.N.; Konoplev, V.N.; Sizareva, A.S.; Aleksandrov, D.P. Peculiarities of the solid-phase formation of strontium pentahydroaluminate from binary hydrides by mechanochemical activation and modeling of the process on the basis of thermogasovolumetry data. *Russ. J. Coord. Chem.* **2000**, *26*, 531–537.
84. Pommerin, A.; Wosylus, A.; Felderhoff, M.; Schüth, F.; Weidenthaler, C. Synthesis, Crystal Structures, and Hydrogen-Storage Properties of Eu(AlH<sub>4</sub>)<sub>2</sub> and Sr(AlH<sub>4</sub>)<sub>2</sub> and of Their Decomposition Intermediates, EuAlH<sub>5</sub> and SrAlH<sub>5</sub>. *Inorg. Chem.* **2012**, *51*, 4143–4150. [[CrossRef](#)] [[PubMed](#)]
85. Kost, M.E.; Golovanova, A.L. Interaction of titanium and iron halides with lithium aluminum hydride in diethyl ether. *Russ. Chem. Bull.* **1975**, *24*, 905–907. [[CrossRef](#)]
86. Weidenthaler, C.; Pommerin, A.; Felderhoff, M.; Sun, W.; Wolverton, C.; Bogdanovic, B.; Schüth, F. Complex rare-earth aluminum hydrides: Mechanochemical preparation, crystal structure and potential for hydrogen storage. *J. Am. Chem. Soc.* **2009**, *131*, 16735–16743. [[CrossRef](#)] [[PubMed](#)]
87. Kost, M.E.; Golvanova, A.I. Reaction of lithium tetrahydroaluminate with transition metal halides. *Inorg. Mater.* **1978**, *14*, 1348–1350.
88. Cao, Z.; Ouyang, L.; Wang, H.; Liu, J.; Felderhoff, M.; Zhu, M. Reversible hydrogen storage in yttrium aluminum hydride. *J. Mater. Chem. A* **2017**, *5*, 6042–6046. [[CrossRef](#)]
89. Claudy, P.; Bonnetot, B.; Bastide, J.-P.; Jean-Marie, L. Reactions of lithium and sodium aluminium hydride with sodium or lithium hydride. Preparation of a new alumino-hydride of lithium and sodium LiNa<sub>2</sub>AlH<sub>6</sub>. *Mater. Res. Bull.* **1982**, *17*, 1499–1504. [[CrossRef](#)]

90. Huot, J.; Boily, S.; Güther, V.; Schulz, R. Synthesis of  $\text{Na}_3\text{AlH}_6$  and  $\text{Na}_2\text{LiAlH}_6$  by mechanical alloying. *J. Alloys Compd.* **1999**, *283*, 304–306. [[CrossRef](#)]
91. Brinks, H.; Hauback, B.; Jensen, C.; Zidan, R. Synthesis and crystal structure of  $\text{Na}_2\text{LiAlD}_6$ . *J. Alloys Compd.* **2005**, *392*, 27–30. [[CrossRef](#)]
92. Løvvik, O.; Swang, O. Structure and stability of possible new alanates. *EPL (Europhys. Lett.)* **2004**, *67*, 607. [[CrossRef](#)]
93. Graetz, J.; Lee, Y.; Reilly, J.; Park, S.; Vogt, T. Structures and thermodynamics of the mixed alkali alanates. *Phys. Rev. B* **2005**, *71*, 184115. [[CrossRef](#)]
94. Sørby, M.; Brinks, H.; Fossdal, A.; Thorshaug, K.; Hauback, B. The crystal structure and stability of  $\text{K}_2\text{NaAl}_6$ . *J. Alloys Compd.* **2006**, *415*, 284–287. [[CrossRef](#)]
95. Bhatnagar, A.; Pandey, S.K.; Shahi, R.R.; Hudson, M.; Shaz, M.; Srivastava, O. Synthesis, characterization and hydrogen sorption studies of mixed sodium-potassium alanate. *Cryst. Res. Technol.* **2013**, *48*, 520–531. [[CrossRef](#)]
96. Rönnebro, E.; Majzoub, E.H. Crystal structure, Raman spectroscopy, and ab initio calculations of a new bialkali alanate  $\text{K}_2\text{LiAlH}_6$ . *J. Phys. Chem. B* **2006**, *110*, 25686–25691. [[CrossRef](#)] [[PubMed](#)]
97. Bulychev, B.; Semenenko, K.; Bitcoev, K. Synthesis and investigation of complex compounds of magnesium alanate. *Koord Khim* **1978**, *4*, 374–380.
98. Grove, H.; Brinks, H.; Heyn, R.; Wu, F.-J.; Opalka, S.; Tang, X.; Laube, B.; Hauback, B. The structure of  $\text{LiMg}(\text{AlD}_4)_3$ . *J. Alloys Compd.* **2008**, *455*, 249–254. [[CrossRef](#)]
99. Grove, H.; Brinks, H.W.; Løvvik, O.M.; Heyn, R.H.; Hauback, B.C. The crystal structure of  $\text{LiMgAlD}_6$  from combined neutron and synchrotron X-ray powder diffraction. *J. Alloys Compd.* **2008**, *460*, 64–68. [[CrossRef](#)]
100. Jain, L.; Jain, P.; Jain, A. Novel hydrogen storage materials: A review of lightweight complex hydrides. *J. Alloys Compd.* **2010**, *503*, 303–339. [[CrossRef](#)]
101. Mohtadi, R.; Sivasubramanian, P.; Hwang, S.-J.; Stowe, A.; Gray, J.; Matsunaga, T.; Zidan, R. Alanate–borohydride material systems for hydrogen storage applications. *Int. J. Hydrogen Energy* **2012**, *37*, 2388–2396. [[CrossRef](#)]
102. Ismail, M.; Zhao, Y.; Yu, X.; Mao, J.; Dou, S. The hydrogen storage properties and reaction mechanism of the  $\text{MgH}_2$ – $\text{NaAlH}_4$  composite system. *Int. J. Hydrogen Energy* **2011**, *36*, 9045–9050. [[CrossRef](#)]
103. Shi, Q.; Yu, X.; Feidenhans'l, R.; Vegge, T. Destabilized  $\text{LiBH}_4$ – $\text{NaAlH}_4$  Mixtures Doped with Titanium Based Catalysts. *J. Phys. Chem. C* **2008**, *112*, 18244–18248. [[CrossRef](#)]
104. Ravnsbæk, D.B.; Jensen, T.R. Tuning hydrogen storage properties and reactivity: Investigation of the  $\text{LiBH}_4$ – $\text{NaAlH}_4$  system. *J. Phys. Chem. Solids* **2010**, *71*, 1144–1149. [[CrossRef](#)]
105. Ismail, M. Study on the hydrogen storage properties and reaction mechanism of  $\text{NaAlH}_4$ – $\text{MgH}_2$ – $\text{LiBH}_4$  ternary-hydride system. *Int. J. Hydrogen Energy* **2014**, *39*, 8340–8346. [[CrossRef](#)]
106. Xia, G.; Tan, Y.; Chen, X.; Guo, Z.; Liu, H.; Yu, X. Mixed-metal (Li, Al) amidoborane: Synthesis and enhanced hydrogen storage properties. *J. Mater. Chem. A* **2013**, *1*, 1810–1820. [[CrossRef](#)]
107. Nakagawa, Y.; Isobe, S.; Ikarashi, Y.; Ohnuki, S. AB–MH (Ammonia Borane–Metal Hydride) composites: Systematic understanding of dehydrogenation properties. *J. Mater. Chem. A* **2014**, *2*, 3926–3931. [[CrossRef](#)]
108. Liu, Y.; Ren, Z.; Zhang, X.; Jian, N.; Yang, Y.; Gao, M.; Pan, H. Development of catalyst-enhanced sodium alanate as an advanced hydrogen-storage material for mobile applications. *Energy Technol.* **2018**, *6*, 487–500. [[CrossRef](#)]
109. Møller, K.T.; Sheppard, D.; Ravnsbæk, D.B.; Buckley, C.E.; Akiba, E.; Li, H.-W.; Jensen, T.R. Complex Metal Hydrides for Hydrogen, Thermal and Electrochemical Energy Storage. *Energies* **2017**, *10*, 1645. [[CrossRef](#)]

